

An urban-based climatology of winter precipitation in the northeast United States

Bradford Johnson*, J. Marshall Shepherd

University of Georgia, Department of Geography, 210 Field St #204, Athens, GA 30602, USA



ARTICLE INFO

Keywords:
Urban climate
Winter
Precipitation
Urbanization
Climatology

ABSTRACT

Varying forms of precipitation during winter weather events cause disruptions to commercial operations and transportation networks, particularly in densely populated regions. Developing a better understanding of the characteristics surrounding these events may lead to better prediction and subsequent mitigation. This study constructs a 21-year cold season climatology of precipitation type over highly urbanized areas of the northeastern United States. By using quality-controlled station reports, a specific focus is placed on the influence of urbanization in precipitation processes. In events involving multiple precipitation types, the ambient atmospheric profile is very close to the freezing point in lower levels. The influence of the boundary layer urban heat island may play a role in increasing melting of hydrometeors. Statistically significant findings from linear regression modeling show that proximity to urban centers, as derived from mean road density, plays a role in the surface observation of mixed precipitation events. 21% of any mixed precipitation observation may be attributed to its distance from a high density urban area. Decreases in mean surface wind speed and direction during mixed precipitation events increase the likelihood of an intact boundary layer urban heat island and melting of hydrometeors when compared to stronger wind speeds during snowfall events.

1. Introduction

Cities are home to more than half of the world's population (United Nations, 2012). Alongside the population increase, the urban footprint on the planet increases. Accompanying high population densities facilitate a rise in societal and infrastructural vulnerability. As urbanization expands and, in many cases, merge with neighboring urban areas, the resilience of these cities to weather and climate phenomena has been a subject of much interest (Klein et al., 2003). This resiliency is especially tested during winter weather events that have paralyzed cities up to several days at a time. Examples in the United States extend from Atlanta, Georgia in January 2014 to Boston, Massachusetts in January 2015 to Washington, DC in December 2016 among many others. Whether due to snow and/or ice, transportation and commercial operations are severely impacted during winter weather events (Maze et al., 2006).

Urban climatology has produced an abundance of research detailing the effects of urbanization on local climate regimes. Seto and Shepherd (2009) summarize this research and find that increases in urbanization change local climates through many factors, including, but not limited to, precipitation distribution, circulation regimes, and the urban heat island (UHI). The heterogeneity of land cover and land use in contiguous urban areas, or urban clusters, may result in greater (and lesser) impacts within, between, and outside of traditional city boundaries. A better understanding of cities' abilities to modify precipitation patterns is of crucial importance to urban planning and resource management. Most studies on urban-precipitation interactions have predominantly focused

* Corresponding author.

E-mail addresses: bdjohns@uga.edu (B. Johnson), marshgeo@uga.edu (J.M. Shepherd).

on warm season impacts because the urbanized signal can more easily be discerned relative to periods dominated by larger-scale forcing (Mitra and Shepherd, 2016). Recent advances in regards to warm-season convection have further strengthened the literature (McLeod et al., 2017). Many mid- and high-latitude cities are also vulnerable to cold-season, winter weather events that potentially cause significant socioeconomic interruptions (Black and Mote, 2015). Climatological and meteorological studies have addressed prediction of winter precipitation. Very few, however, focused on the effects of urbanization on winter precipitation. Even fewer have addressed the role of urban clusters on transitional aspects of winter precipitation. Hereafter, *transitional* refers to any event where multiple precipitation types have been observed at the surface. Forecasting of transitional events remains difficult (Schuur et al., 2012). Compounding the difficulty, urban areas have the ability to alter the lower atmospheric temperature and moisture profiles through anthropogenic activities (Oke, 1995; Taha and Bornstein, 1999). Consequently, observed precipitation may not be consistent with the anticipated precipitation type considering the nearest observed or modeled atmospheric sounding profile.

Urbanization may not only lead to winter precipitation modification but also precipitation initiation or enhancement. Shepherd and Mote (2011) provide an example of this in a January 2011 case study in Dodge City, Kansas. Byproducts of local industrial activities (aerosols, excess water vapor, and heat) were advected by southeasterly surface winds into the lower atmosphere. The resulting plume served as a catalyst for snowfall downwind of the facilities into and northwest of the city.

This paper investigates the impact of urban clusters on precipitation type by constructing a winter season climatology and considering the urban morphology. Can urbanization alter the atmospheric profile enough to influence precipitation type at the surface? Do certain regions within a major urban cluster experience specific types of winter precipitation more or less frequently when compared to adjacent areas? Section 2 discusses the background and considerations made in addressing the objective. Section 3 outlines the data utilized throughout and the domain studied. Section 4 details the methodology and tools applied. Section 5 describes the findings and results, while Section 6 argues the significance of conclusions derived from the study and considers potential impacts and future investigations.

2. Background

Lower atmospheric temperature modifications are caused by urban land use and land cover change and the corresponding changes in the energy balance. The scales of vertical influence are categorized as the surface, canopy, and boundary layer heat islands (Arnfield, 2003). The surface UHI is observed in increased skin temperature primarily due to direct absorption of incoming shortwave and longwave radiation; the canopy UHI extends to roof level and is sustained through the reemission of longwave radiation from the surface and built environment. The urban boundary layer heat island begins above roof level and alters the atmospheric profile up to a kilometer above the surface and for several kilometers downstream (Oke, 1995). As hydrometeors fall through this environment, they encounter relatively warmer temperatures and lower humidity causing increased rates of melting and evaporation. Changnon (2003) found that UHI effects resulted in 0.5 to 2 fewer days on average of freezing rain reports in-city compared to surrounding rural environments in New York City and Chicago. The modification of freezing rain is caused by higher surface temperatures in cities. Clinton and Gong (2013) developed techniques using Moderate Resolution Imaging Spectroradiometer (MODIS) imagery to detect heat sources and sinks within the urban environment by deriving the surface skin temperature. The usefulness of satellite remote sensing like MODIS to obtain surface temperature is limited, however, by cloud cover during synoptic events. This drawback may be alleviated by the use of road sensor network data available through state and regional transportation departments. Measurement of the surface UHI is still useful, particularly for freezing rain, but is not effective for assessing modification of precipitation above the surface.

Stewart and King (1987) outline how precipitation type varies according to hydrometeor diameter, thickness of the freezing layer aloft, and the height of the freezing layer. Therefore, precipitation type prediction is possible if sufficient upper air observations are available. While assessing the viability of precipitation type algorithms designed to predict surface observations, Reeves et al. (2014) notes horizontal nonuniformity in crowd-sourced mPING observations of snow, ice pellets, and freezing rain may be due in part to UHI effects. The lack of upper atmospheric temperature and humidity observations limit the ability to apply implicit algorithms that assess precipitation type. Atmospheric sounding profiles provide data necessary to predict what we *should* observe at the surface then compare this to what actually *is* observed at Automated Surface Observing System (ASOS) sites. Sounding sites are typically on the order of several hundred kilometers apart and are collected every 12 h (Fig. 1b) (National Oceanic and Atmospheric Administration, 2017a). Use of this data is not suitable for spatial analysis on the urban scale nor for temporal analysis of transitional events. Reanalysis datasets, such as the North American Regional Reanalysis (NARR) which has a horizontal resolution of 32 km, 29 vertical levels, and three-hourly temporal resolution, provide acceptable temporal and spatial resolutions (Mesinger et al., 2006). Interpolation on this scale may be meaningful if data model quality is consistent with observations.

An assessment of the viability of NARR data for the purposes of this investigation is necessary. Preliminary analysis of a transitional event on 5 December 2009 highlights potential issues with this approach. Fig. 2 shows discrepancies between the NARR precipitation type algorithm and observed precipitation at ASOS stations. Furthermore, a statistical comparison of NARR data and atmospheric sounding data from two stations located within the affected domain (IAD and OKX, see Fig. 1b) is performed. NARR data is obtained from the grid points corresponding to the geolocation of the sounding stations. Air temperature, geopotential height, and wind speed are extracted from both datasets at 12 UTC on 5 December 2009. Nine standard vertical levels from 100 hPa to 1000 hPa are analyzed. Both, the NARR and sounding data are treated with the assumption of statistical dependence. This is based on principles related to Tobler's First Law of Geography (Tobler, 2004). The data are drawn from the same day and time, from locations < 500 km apart.

Table 1 shows the results of the traditional statistical measures performed. All variables either approached significance or were

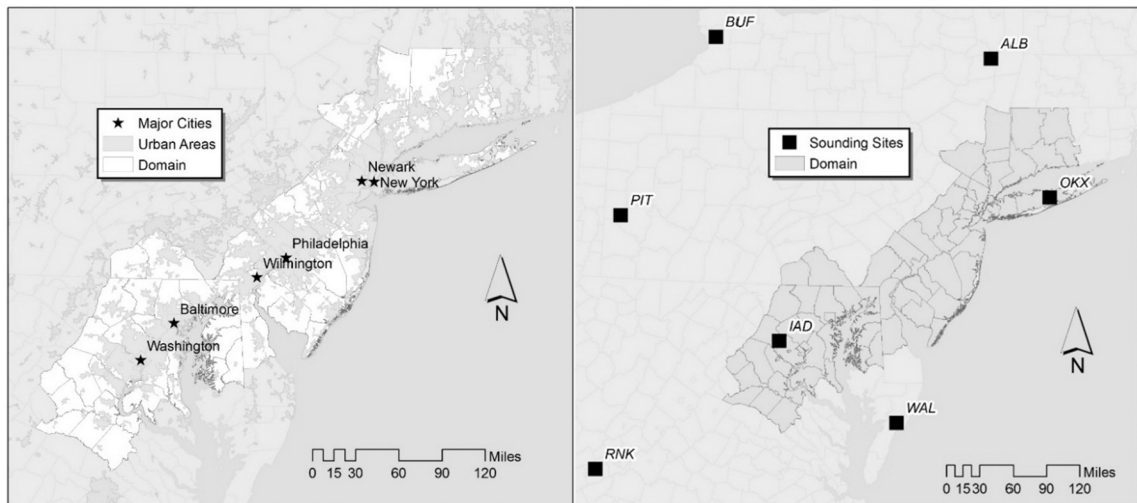


Fig. 1. a) Domain of study, major cities, and regional urban footprint (*left*), and b) NOAA-operated atmospheric sounding sites over the Mid-Atlantic region in the northeastern United States (*right*).

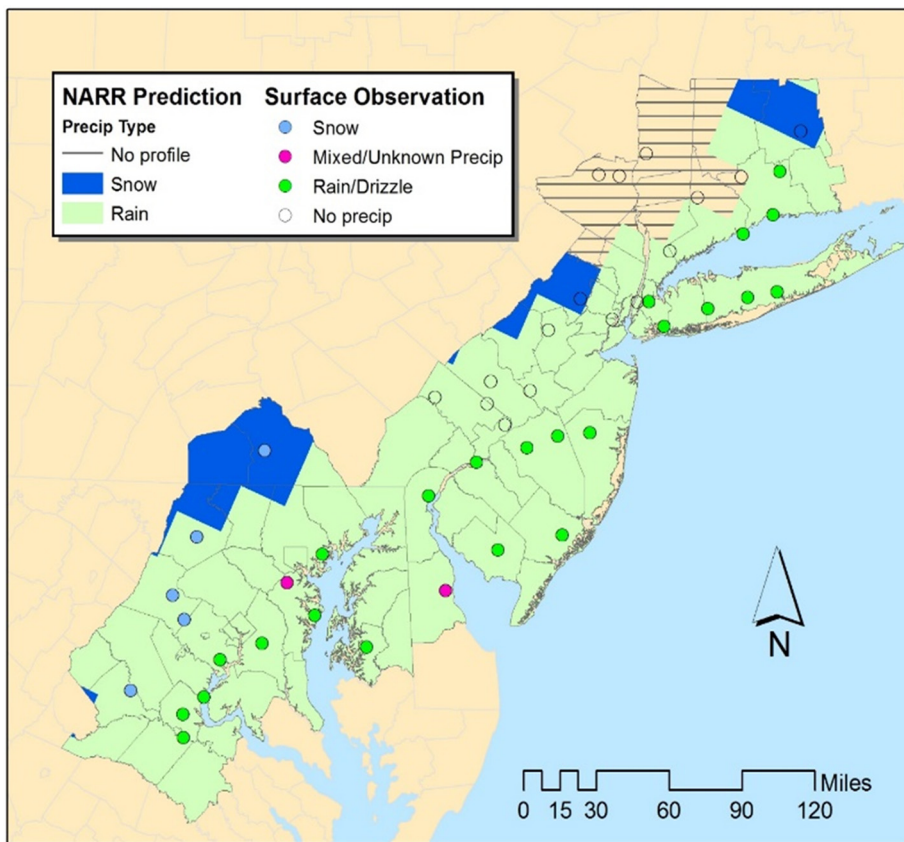


Fig. 2. Validated surface observations versus predicted precipitation from NARR algorithms on 5 December 2009 at 15 UTC.

significantly different from a normal distribution. Since the traditional student's *t*-test could not be performed, a nonparametric technique is utilized. The results of Wilcoxon ranked sum tests, which is designed to tell if two samples are statistically the same (H_0), for each variable reveal inconsistent findings. The NARR and sounding temperature profiles returned a *p*-value equal to 0.08. While the null hypothesis may not be rejected with 95% confidence, it approaches significance. The null hypothesis is accepted for wind speeds. H_0 is rejected for geopotential height, however. A *p*-value of 0.03 indicates the samples are significantly different. While this is a sample case, it highlights the potential inaccuracies introduced through the use of reanalysis in construction of a climatology.

Table 1

Results of statistical testing of upper air data from the IAD and OKX sounding locations and the corresponding NARR grid point for each location. Data is taken on 5 December 2009 at 12 UTC.

Upper air variable	Shapiro-Wilk normality test (p-value)		Wilcoxon signed rank test (p-value)
	Sounding	NARR	
Dry bulb temperature	0.008	0.011	0.081
Wind speed	0.042	0.031	0.212
Geopotential height	0.056	0.056	0.027

[Thériault et al. \(2010\)](#) notes that changes in temperature and dewpoint as small as 0.5 K have been shown to alter precipitation type. This magnitude of anomaly is often observed within the urban boundary layer. With such a small margin for error, construction of a climatology based on available upper atmospheric data is not reasonable.

3. Data and domain

The study domain encompasses the urban cluster from Washington, DC to New York, New York metro areas and adjacent rural areas. The temporal range covers a 21-year period during the cold season (November to April) from 1995 to 2016. Station data for 46 locations from northern Virginia to central Connecticut are obtained from the National Centers for Environmental Information Quality Controlled Local Climatological Data (QCLCD) Hourly (10A) dataset ([NCEI, 2017](#)). It is comprised of standard hourly METARS and intra-hourly specials, or SPECI. Each reporting station from the dataset with continuous 24-h coverage is included. These stations are depicted in [Fig. 3](#). Geospatial data including state, county, and road shapefiles from the United States Census are utilized ([US Census Bureau, 2015](#)).

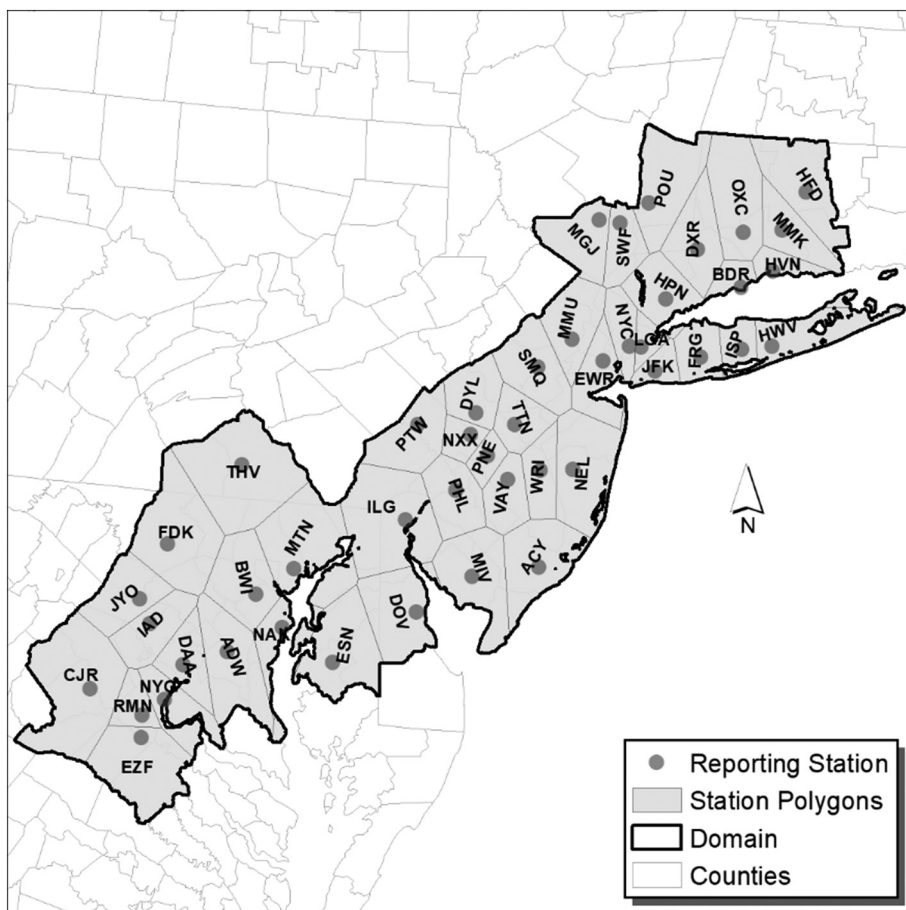


Fig. 3. Surface weather reporting stations with station identifiers and corresponding Thiessen polygons. Data provided by National Centers for Environmental Information (NCEI).

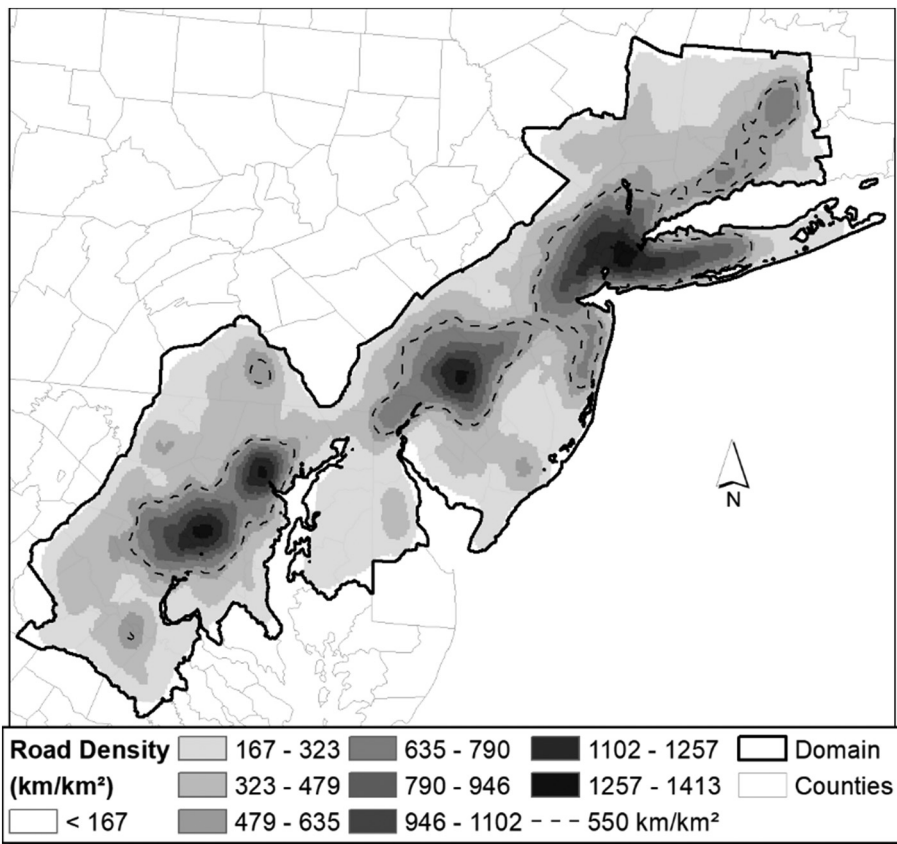


Fig. 4. Domain road density (km/km^{-2}). Derived from United States Census 2014 Topologically Integrated Geographic Encoding and Referencing (TIGER) dataset.

Table 2

Top five days of precipitation by number of individual reports during cold season (November to April) from 1995 to 2016. (Table 3.)

Rank	Date	Total reports	Rain	Snow	Mixed/unknown
1	2007-04-15	1248	1220	1	27
2	2007-03-16	1091	251	121	719
3	2014-12-01	1053	278	758	17
4	2015-12-06	1046	195	800	51
5	2013-12-06	1010	916	70	24

Table 3

Top five days as sorted by combined mixed and unknown precipitation reports during cold season from 1995 to 2016. *Liquid precipitation ratio* (LPR) is the proportion of rain reports to all precipitation reports.

Rank	Date	Total reports	Rain	Snow	Mixed/unknown	LPR
1	2007-03-16	1091	251	121	719	0.23
2	2007-02-14	668	46	58	564	0.07
3	2004-02-06	696	328	39	329	0.47
4	2013-12-08	778	99	377	302	0.13
5	2015-03-01	537	6	273	258	0.01

4. Methodology

Cortinas Jr. et al. (2004) constructed a detailed, observation-based winter precipitation type climatology over the United States and Canada. They highlighted maxima of varying transitional precipitation over the eastern portion of the continent from December to March. Similarly, a station-based climatology of winter precipitation is constructed in this study but with the intent of investigating the potential effect of urbanization. QCLCD files are available per station per month. Two stations, Shannon Airport (EZF) and

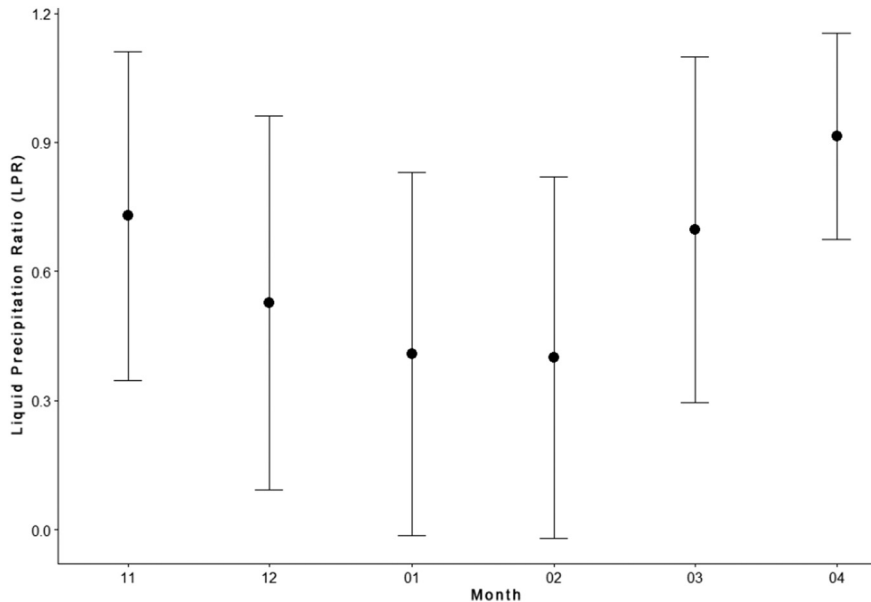


Fig. 5. Mean liquid precipitation ratio (LPR) and associated standard deviation sorted by month from 1995 to 2016.

Easton/Newnam Field Airport (ESN), met the continuous reporting requirement but are available in the dataset from November 2007 to April 2016. Using Python scripting, the QLCD files are merged with station metadata and aggregated into a single 46-station database. Reports that are flagged by NCEI, inconsistent, or included non-standard METAR/SPECI coding are omitted. Each individual report is categorized into rain/drizzle (RA), snow (SN), mixed precipitation/frozen pellets (MX), unknown precipitation (UP), and no precipitation (NA). Using ESRI's ArcGIS platform, each station geolocation will be used to develop Thiessen polygons. These polygons serve as tools to visually conceptualize the space surrounding each reporting station (Fig. 3) (Shepherd et al., 2014).

Atmospheric variables of temperature, dewpoint, wind speed, wind direction, and mean sea level pressure are available hourly and occasionally sub-hourly. At each station, the following aggregate statistics are computed:

- Monthly over the temporal span
 - Percentage/total reports of RA
 - Percentage/total reports of SN
 - Percentage/total reports of MX
 - Percentage/total reports of UP
 - Mean atmospheric variables
- Over the entire temporal span
 - Percentage/total reports of RA
 - Percentage/total reports of SN
 - Percentage/total reports of MX
 - Percentage/total reports of UP
 - Mean atmospheric variables

To determine if an urban bias exists, the proportionalities will be incorporated into spatial analysis using ArcGIS and R statistical software package. The National Land Cover Database (NLCD) provides a spatially fine, heterogeneous representation of surface land cover. Several reporting stations are in urban-rural transition zones, or areas under going gradual transition from majority rural land cover to impervious surfaces. Assigning a single surface land cover type to each polygon requires aggregation of the NLCD data, neutralizes its spatial advantage, and diminishes its usability. Road network density varies gradually and is more indicative of urbanization on the scale of interest here. Fig. 4 shows road density as calculated from 2014 US Census Topologically Integrated Geographic Encoding and Referencing (TIGER) dataset and serves as a proxy for urbanization (McKinney, 2002). Road density is partitioned into two categories – URBAN and RURAL – where road density is greater than or equal to 550 km/km^2 or $< 550 \text{ km/km}^2$, respectively. These thresholds were established to qualitatively represent the regional urban form and provide spatial footprints large enough to include a sufficient number of associated reporting stations. URBAN is considered dense urban, sparse urban, and suburban subcategories; RURAL encompasses ex-urban and rural. This categorization and other geographical variables including elevation, latitude, proximity to coastline are considered in combination with the atmospheric variables.

Table 4

Fourty-six domain reporting stations utilized in the study. All data obtained from NCEI Quality Controlled Local Climatological Data Hourly 10A dataset.

WBAN	Lat (°)	Lon (°)	ID	Name	Elevation (m)	Precip count
4781	40.793	-73.101	ISP	LONG ISLAND MAC ARTHUR ARPT	25.6032	5166
13,739	39.868	-75.231	PHL	PHILADELPHIA INTL AIRPORT	3.048	7802
13,773	38.5	-77.3	NYG	QUANTICO MCAF	3.048	4357
13,781	39.672	-75.6	ILG	NEW CASTLE COUNTY ARPT	24.0792	5555
14,732	40.779	-73.88	LGA	LA GUARDIA ARPT	3.3528	5417
14,734	40.682	-74.169	EWR	NEWARK LIBERTY INTL ARPT	2.1336	5611
93,721	39.166	-76.683	BWI	BALTIMORE-WASHINGTON INTL ARPT	47.5488	4959
93,730	39.449	-74.567	ACY	ATLANTIC CITY INTL AIRPORT	18.288	4732
93,738	38.94	-77.463	IAD	WASHINGTON DULLES INTL AP	88.392	5002
94,702	41.158	-73.128	BDR	IGOR I SIKORSKY MEMORIAL ARPT	1.524	6094
94,728	40.778	-73.969	NYC	CENTRAL PARK	39.624	4748
94,732	40.081	-75.011	PNE	NE PHILADELPHIA AIRPORT	30.48	6691
94,789	40.638	-73.762	JFK	JOHN F KENNEDY INTL ARPT	3.3528	5019
14,793	40.2	-75.15	NXX	WILLOW GROVE NAS	110.0328	3208
14,752	41.736	-72.65	HFD	HARTFORD-BRAINARD ARPT	5.7912	5606
93,778	39.918	-76.874	THV	YORK ARPT	148.1328	5283
93,780	39.949	-74.841	VAY	SOUTH JERSEY REGIONAL ARPT	16.1544	5259
4789	41.509	-74.265	MGJ	ORANGE COUNTY ARPT	111.252	5336
14,792	40.276	-74.815	TTN	TRENTON MERCER ARPT	56.0832	5018
54,734	41.371	-73.482	DXR	DANBURY MUNICIPAL ARPT	139.2936	6183
13,735	39.366	-75.066	MIV	MILLVILLE MUNICIPAL ARPT	21.336	4872
54,782	40.238	-75.557	PTW	POTTSTOWN LIMERICK ARPT	88.6968	4550
14,780	40.033	-74.35	NEL	NAES/MAXFIELD FIELD	30.7848	2042
54,785	40.623	-74.669	SMQ	SOMERSET ARPT	32.004	3707
54,786	40.33	-75.122	DYL	DOYLESTOWN ARPT	120.0912	4677
54,787	40.734	-73.416	FRG	REPUBLIC ARPT	24.6888	4505
54,788	41.509	-72.827	MMK	MERIDEN MARKHAM MUNI ARPT	31.3944	5519
54,790	40.821	-72.868	HWV	BROOKHAVEN ARPT	24.9936	5381
14,757	41.626	-73.884	POU	DUTCHESS COUNTY ARPT	50.5968	4328
94,745	41.066	-73.707	HPN	WESTCHESTER COUNTY ARPT	115.5192	2707
14,758	41.263	-72.887	HVN	TWEED-NEW HAVEN ARPT	0.9144	4080
3706	38.266	-77.449	EZF	SHANNON ARPT	25.908	7870
3714	39.077	-77.557	JYO	LESSBURG EXECUTIVE ARPT	118.5672	9017
13,730	39.416	-77.383	FDK	FREDERICK MUNICIPAL ARPT	92.3544	8123
64,707	41.483	-73.133	OXC	WATERBURY-OXFORD ARPT	221.2848	553
93,744	39.333	-76.416	MTN	MARTIN STATE ARPT	6.4008	4665
93,798	38.526	-77.858	CJR	CULPEPPER REGIONAL ARPT	96.3168	9793
3735	38.398	-77.455	RMN	STAFFORD REGIONAL ARPT	64.6176	10,116
13,707	39.133	-75.466	DOV	DOVER AFB ARPT	8.5344	8511
13,752	38.983	-76.466	NAK	U.S. NAVAL ACADEMY	2.4384	2983
93,728	38.716	-77.183	DAA	DAVISON AAF ARPT	22.2504	7675
54,738	40.8	-74.416	MMU	MORRISTOWN MUNICIPAL ARPT	56.9976	4242
13,705	38.816	-76.866	ADW	ANDREWS AIR FORCE BASE ARPT	85.9536	8456
14,706	40.016	-74.6	WRI	MCGUIRE AFB ARPT	39.9288	10,148
14,714	41.5	-74.1	SWF	STEWART INTL ARPT	149.6568	1177
3756	38.804	-76.068	ESN	EASTON/NEWNAM FIELD ARPT	21.9456	3662

5. Results and discussion

3277 total days were analyzed over the domain from November to April from Fall 1995 to Spring 2016. 4,117,199 unique station reports were included. The breakdown of raw precipitation reports by binned type over the entire temporal span is as follows.

- RA – 172,794
- SN – 54,472
- MX – 6908
- UP – 15,961
- NA – 3,866,771

2262 days were recorded with at least one precipitation report. Of these days, 192 included exactly one precipitation report domain-wide; 2070 days had multiple precipitation reports. The maximum number of daily precipitation reports (1248) occurred on 2007 April 15 (Table 2). 250,428 station reports include some form of precipitation. Table 2 lists the dates with the most MX and UP. Table 3 introduces the liquid precipitation ratio (LPR) shown below,

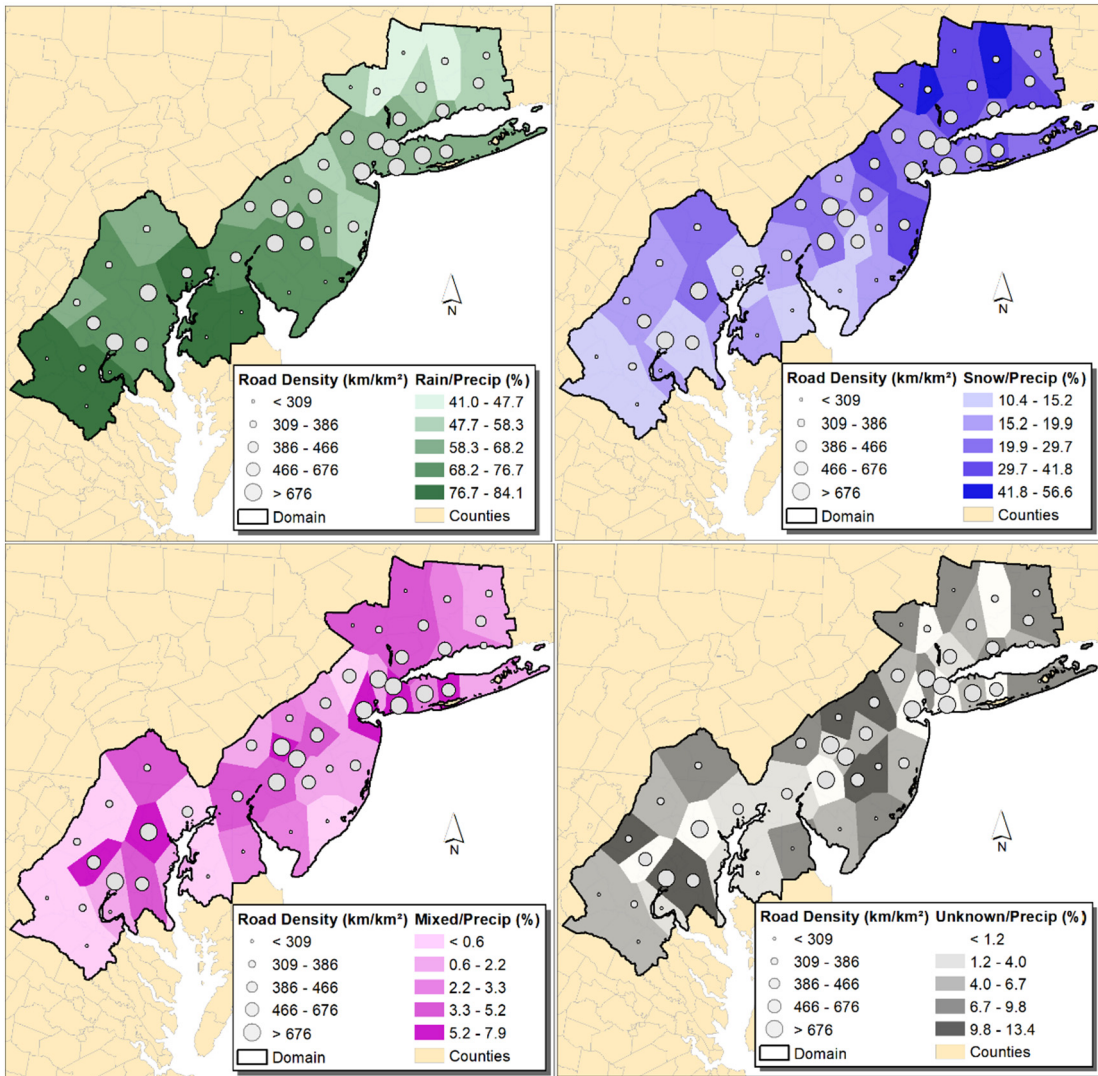


Fig. 6. Ratio of reported precipitation type – rain (top left), snow (top right), mixed precipitation (bottom left), and unknown precipitation (bottom right) – to all precipitation reports by station polygon. Mean polygon road density is also shown. Derived from NCEI Quality Controlled Local Climatological Data Hourly 10A dataset. Basemap data derived from US Census.

$$LPR = RA \cdot AP^{-1}, \quad (1)$$

where RA is the number of rain reports and AP is the number of total precipitation reports. LPR gauges the seasonal nature of the regional precipitation. An LPR equal to 1 means no winter precipitation is present over the domain while values closer to zero denote increasing reports of winter weather relative to rainfall. Fig. 5 shows LPR minima occur during the months of January and February. Large variance is present from November to March indicating a wide range of year-to-year variability in frozen precipitation ratios.

Table 4 details the geographical attributes and aggregate precipitation report counts for each station. Fig. 6 displays the distribution of precipitation types by Thiessen polygon. Opposite latitudinal trends are evident in RA and SN distributions with greatest frequencies in the south and north, respectively. Similar distributions are not present in reported MX and UP types. Fig. 7 removes RA which accounts for 69.0% of all precipitation reports and provides a ratio of reported MX and UP types by station. A few features are notable. 1) The northern latitudinal tilt toward snowfall is reinforced, 2) there is no discernible coastal effect, and 3) several southern stations, particularly near the Washington, DC metro and Chesapeake Bay, observe similar totals of snowfall events when compared to a combination of mixed and unknown events. An example of the latter point is Andrews Air Force Base (ADW) where 992 SN reports are recorded compared to 1299 combined MX (316) and UP (983) reports.

Mixed and unknown reports both lack clear spatial trends in overall precipitation distribution. Since UP reports are often unverifiable away from augmented sites, the conditions under which a report returns unknown is needed. Four stations do not report any MX over the entire temporal span and collectively account for 14.7% of all reports (Fig. 8). The lack of reports is likely not due to the absence of MX rather than limited detection capabilities of the automated sensors (National Oceanic and Atmospheric

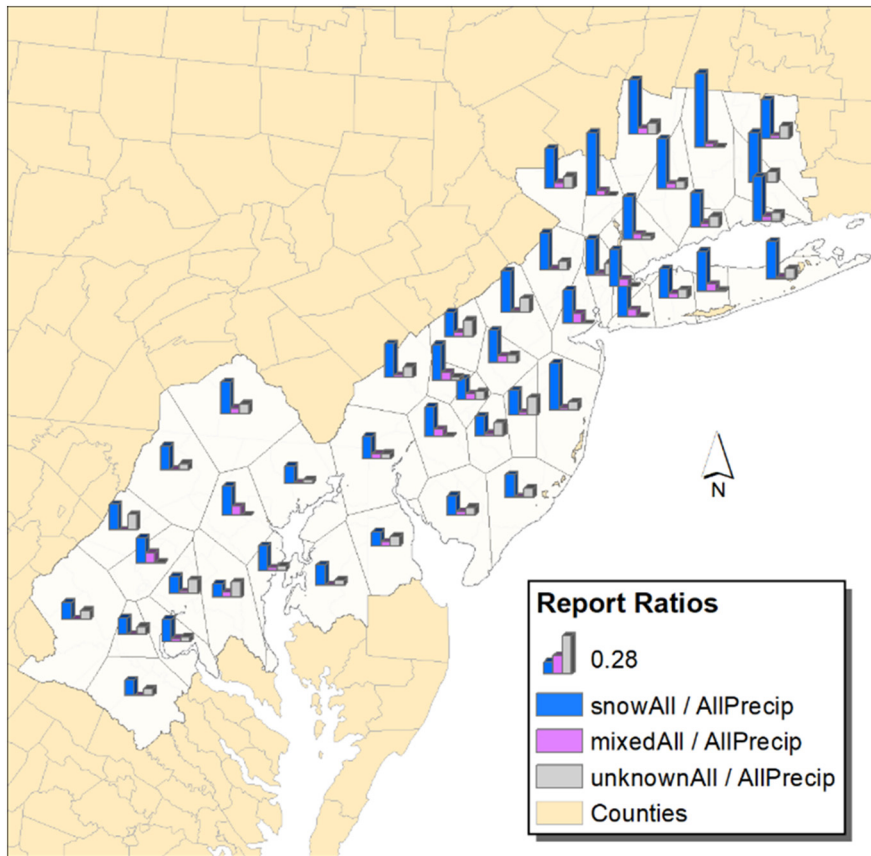


Fig. 7. Ratio of reported precipitation type to all precipitation reports by station excluding rain reports.

(Administration, 1998). Consequently, these stations are omitted from further analysis resulting in consideration of 42 reporting stations. This adjustment reduces the total number of reports by 497,701 and precipitation reports by 36,819; no change is noted in total MX reports. Precipitation type totals and associated atmospheric variables are aggregated for all 42 stations. Further analysis is based upon the aggregated station data unless otherwise noted. Fig. 9 shows relationships of station temperature for all four precipitation categories. The domain-wide, station aggregate mean temperatures during RA and SN events are 8.22 °C and – 2.83 °C, respectively, while the standard deviations are 0.67 °C and 0.89 °C. Mean temperature during MX events is – 0.54 °C with a standard deviation of 0.72 °C; UP mean temperature is 1.47 °C with a standard deviation of 1.48 °C. Visual inspection and normality testing of temperature histograms warrant nonparametric analysis (not shown). Mann Whitney U tests of the six precipitation type relationships (i.e. MX-RN, SN-UP, etc.) are performed with a null hypothesis, h_0 , of equal temperature means. All combinations return $p \ll 0.05$ and reject h_0 MX and UP where $p = 0.59$ and h_0 may be accepted. The temperature distributions of both mixed and unknown populations are equal. This reinforces the visual interpretation of Fig. 9 that shows the similarity between MX and UP and the differences between other combinations. These analyses suggest that many UP are mixed precipitation in reality. Considering the mean is close to the freezing point and the lower end of UP standard deviation falls below the freezing point, this is entirely probable. While reports at or below 0 °C may be attributed to some form of freezing precipitation with high confidence, UP at higher temperatures may not have any associated frozen components. The data is not sufficient to assign all UP as mixed precipitation. For this reason, a combined MX and UP category has limited statistical usefulness beyond the descriptive measures previously described.

Surface wind speed, u , and direction over the domain suggest synoptic forcing, storm track, and storm intensity play a key role in transitional events. During the cold season, the mean overall wind direction is from the northwest (333.4°) domain-wide (Table 5, Fig. 10). Wind roses separated by precipitation type and derived from individual reports are displayed in Fig. 11. The predominant wind directions by precipitation type rotate from northerly to northeasterly in the order of SN (357.5°), UP (7.3°), RA (22.9°), and MX (30.5°). The correlating mean wind speeds, \bar{u} , in meters per second are 6.3, 5.6, 5.3, and 5.6, respectively. Furthermore, u is useful in determining the impact of urbanization on atmospheric temperature profile. Oke (1995) states that strong boundary layer UHIs may remain intact at $u < 5 \text{ ms}^{-1}$, or approximately 10 knots. Table 5 shows the ratios of SN and MX exceeding this threshold are 0.65 and 0.57, respectively. In comparison with snowfall events, this 8% decrease in \bar{u} during mixed precipitation events supports the criteria necessary to sustain warmer temperatures near the surface. Weaker, northeasterly winds during MX events are indicative of a position north of warm fronts. The stronger, northerly winds observed during SN events are common in regions of strong cold air advection on the western side of low pressure centers. In an environment of decreased wind speeds and near freezing temperatures in

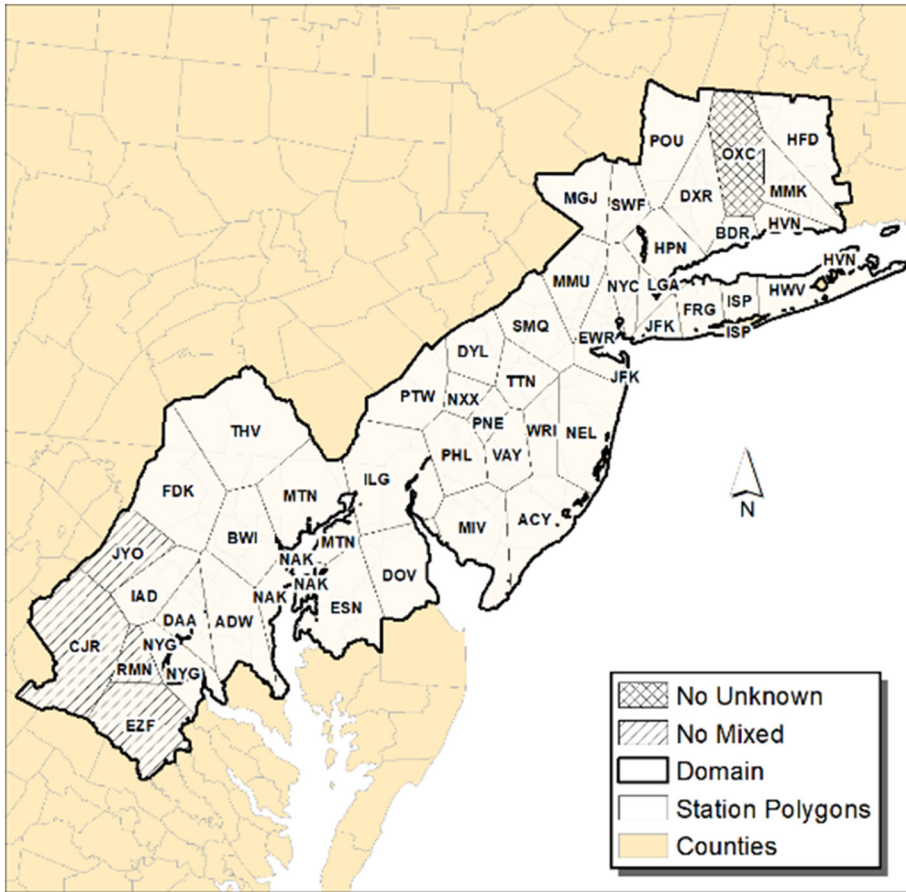


Fig. 8. Reporting stations with no mixed or unknown precipitation reports over the entire temporal span.

the lower troposphere, further thermal perturbations by an entrenched UHI would support transition of hydrometeors.

Understanding the variance and characteristics of precipitation type domain-wide is useful but insufficient in determining the urban influence on transition. Urban morphologies vary on different scales. Cities differ from neighboring cities; the same holds true from region to region and country to country. According to Luck and Wu (2002), the urban density decreases in a gradient-like pattern from the city center. While land use types are heterogeneous, they generally follow an urban/suburban/ex-urban/rural progression. The URBAN and RURAL road density categorization is utilized to determine how precipitation evolves across these boundaries. The reported counts of precipitation type at each station are compared to their respective URBAN/RURAL designation. For example, KADW has a classification of URBAN and a snowfall report count of 879. This is compared to the snowfall count at the other reporting stations considering their respective urban categorization. Sample code of the Wilcoxon rank sum test in the R statistical package for this example is.

$$\text{wilcox. test}(s \sim UC, \text{data} = df), \quad (2)$$

where s is snow reports by station, UC is the urban categorization by station, and df is the dataframe containing all aggregated station data. The null hypothesis, h_0 , proposes that the distribution of each respective precipitation type is similar between both URBAN and RURAL stations. Of the four precipitation categories, only MX returned significant results ($p \approx 0.002$), rejecting h_0 . This result implies (greater than a 99% chance) a significant difference between the number of MX in urban and rural areas exists. It does not assign causation nor define a polarity to the difference. These findings are also confirmed through additional analysis following the Kruskal-Wallis rank sum technique (not shown). Related analysis for UP returned $p \approx 0.08$ suggesting findings approach but do not meet a 95% confidence level.

Regression models are constructed to ascertain the direction of the relationship between precipitation type and mean road density (Fig. 12). The linear models compare the number of precipitation reports, N , by reporting station to the mean road density of each corresponding Thiessen polygon and are performed monthly over the temporal span. No significant relationship is apparent for RA, SN, and UP. The MX regression models in Fig. 12C and Fig. 13 highlight 1) a positive relationship between MX and mean road density, 2) significant findings with > 99% confidence over the period, 3) significant findings > 95% confidence in the months of November, January, February, March, and April, and 4) an attribution of 21% by mean road density to MX occurrences. Through histogram inspection and Kolmogorov-Smirnov testing, the residuals represent a normal distribution. URBAN sites observed 3854 MX

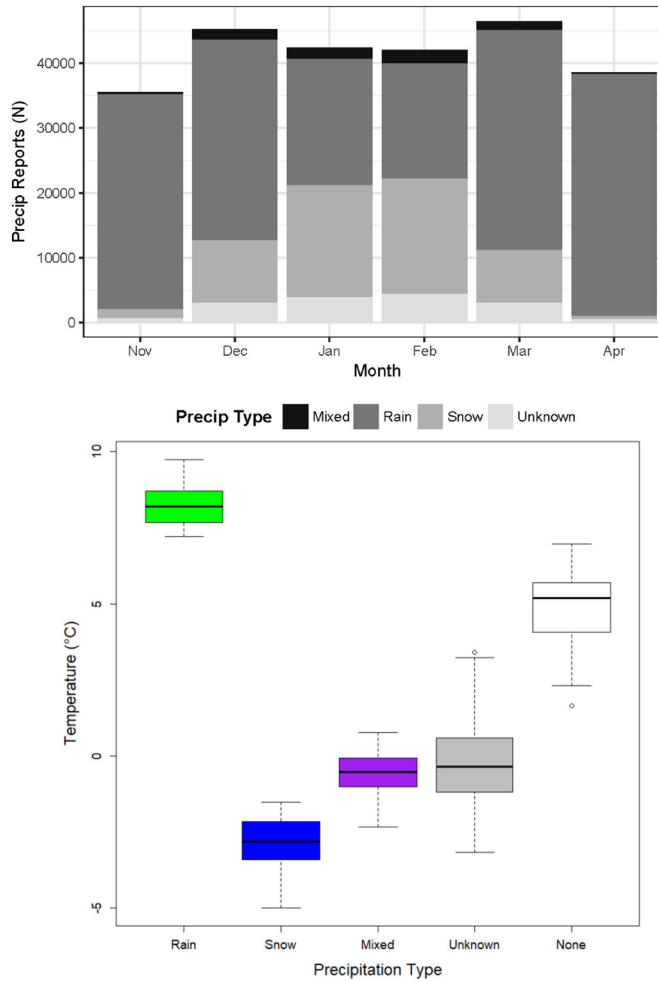


Fig. 9. (top) Gross monthly count of precipitation reports by type from 1995 to 2016. (bottom) Mean surface temperature ($^{\circ}\text{C}$) coincident with each observed precipitation type.

Table 5

Total number of reports, N , including a valid wind speed, u , mean wind speed, \bar{u} , and wind direction for each precipitation type. Standard deviations, σ , show variance of wind speed distributions. $\text{Reports}_{(u > 5 \text{ ms}^{-1})} \cdot N^{-1}$ is the ratio of reports for each precipitation type exceeding the boundary layer UHI threshold (Oke, 1995).

Precip type	N, u Reports	\bar{u} (kt) [ms^{-1}]	Standard deviation, σ (kt) [ms^{-1}]	Ratio exceeding 5 ms^{-1}	Mean wind direction ($^{\circ}$)
All precip	2,371,559	8.62 [4.44]	5.37 [2.77]	0.39	333.4
Snow	28,450	12.3 [6.32]	4.93 [2.54]	0.65	357.5
Mixed	4544	10.9 [5.58]	5.21 [2.68]	0.57	30.5
Rain	90,485	10.9 [5.25]	5.08 [2.61]	0.55	22.9
Unknown	9322	10.2 [5.63]	6.02 [3.10]	0.50	7.34
No precip	2,238,741	8.47 [4.36]	5.35 [2.75]	0.38	331.0

(~ 11.5 reports per station per year), RURAL sites reported 3054 MX occurrences (~ 5.6 reports per station per year).

6. Conclusion

This study details a 21-year, reporting station-based, cold season climatology of winter precipitation type over the northeastern United States from northern Virginia to western Connecticut. Synoptic scale systems that produce a variety of liquid and frozen precipitation frequently traverse the region. As the margins in temperature and dewpoint during transitional events are very small, precision is of the utmost importance. Spatial and temporal limitations on observational and reanalysis data inhibit traditional

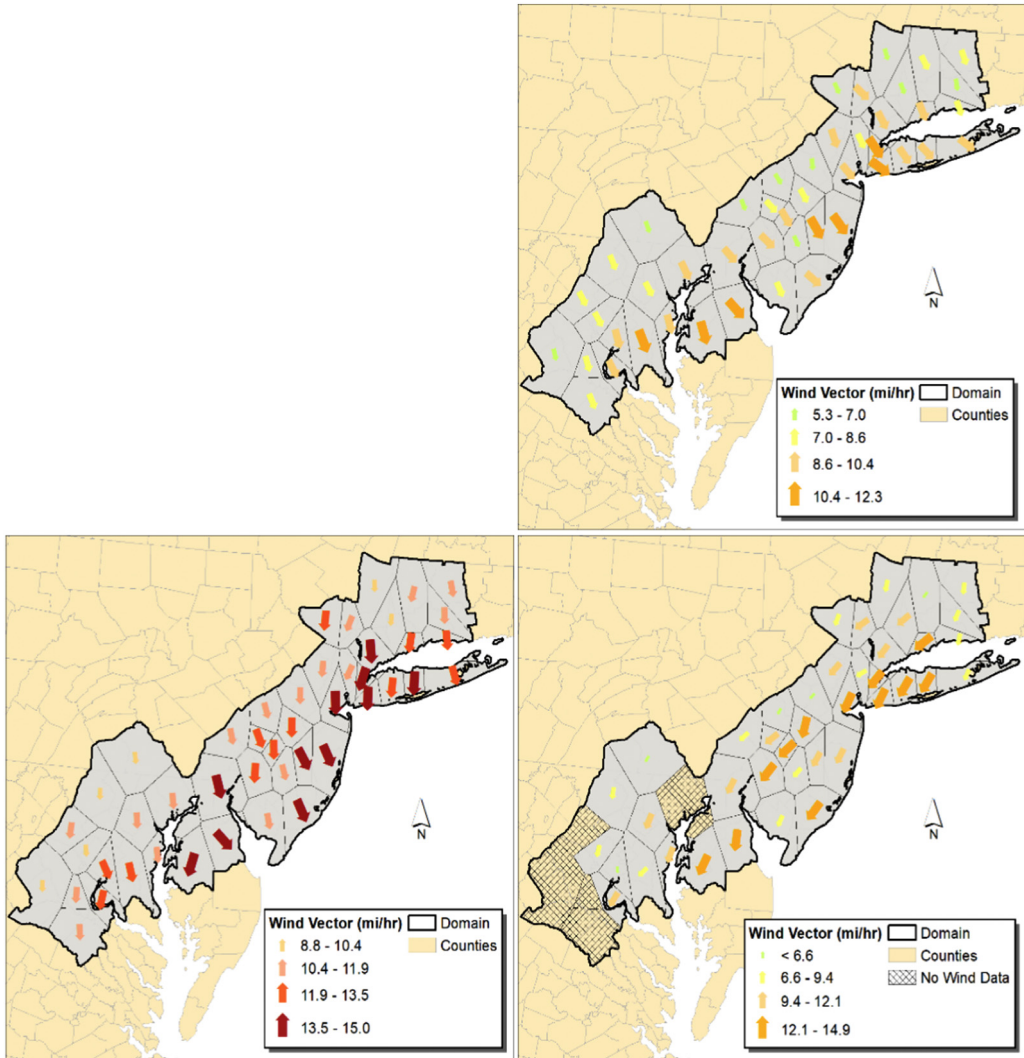


Fig. 10. (top) Mean surface wind, \bar{u} , for all observations at each reporting station from November 1995 to April 2016. (left) Same as top, but for all snow observations. (right) Same as top, but for all mixed precipitation observations.

investigation of upper atmospheric and synoptic-scale drivers of precipitation type. However, the robust station data ($N > 4.1$ million reports) provide insight on the phenomena and the potential anthropogenic influences.

An emphasis is placed on the relationship between transitional precipitation and the urban environment. Through a net positive radiative heat budget in urban areas, cities develop warm anomalies in the lower atmosphere. When synoptic conditions are marginally conducive to winter precipitation, these anomalies may supply enough heat to alter the phase state of falling hydrometeors. *Statistically significant findings show that proximity to urban centers, as derived from mean road density, plays a role in the surface observation of mixed precipitation events.* 21% of any mixed precipitation observation may be attributed to its distance from a high density urban area. As road density increases, mixed precipitation reports increase. *On average, urban areas reported approximately six more instances of mixed precipitation per year.*

While these observation-based findings are encouraging, there are considerations that must be accounted for when attributing precipitation modification to urbanization. The use of observations is the most accurate representation of reality available. ASOS observations provide a dense spatial and temporal data source but have difficulty accurately reporting frozen pellets. This results in many unknown precipitation reports where ASOS observations are not augmented by human observers (Reeves, 2016). Additionally, the likelihood of human observers being present is higher at urban sites (i.e. staffed facilities) than rural sites. This is the driving factor behind limiting the precipitation type bins to mixed and unknown categories instead of individual precipitation types. In fact, *Cortinas Jr. et al., 2004* limited their climatology to before 1990 to eliminate ASOS data from analysis. The close statistical relationship between mixed and unknown reports is a result of the current observational restraints. Determining if the relationship between mixed precipitation and urbanization is legitimate will depend, in part, on the relationship between augmented observation sites, the probability of detection at ASOS sites, and proximity to urban areas. These observational limitations are well established

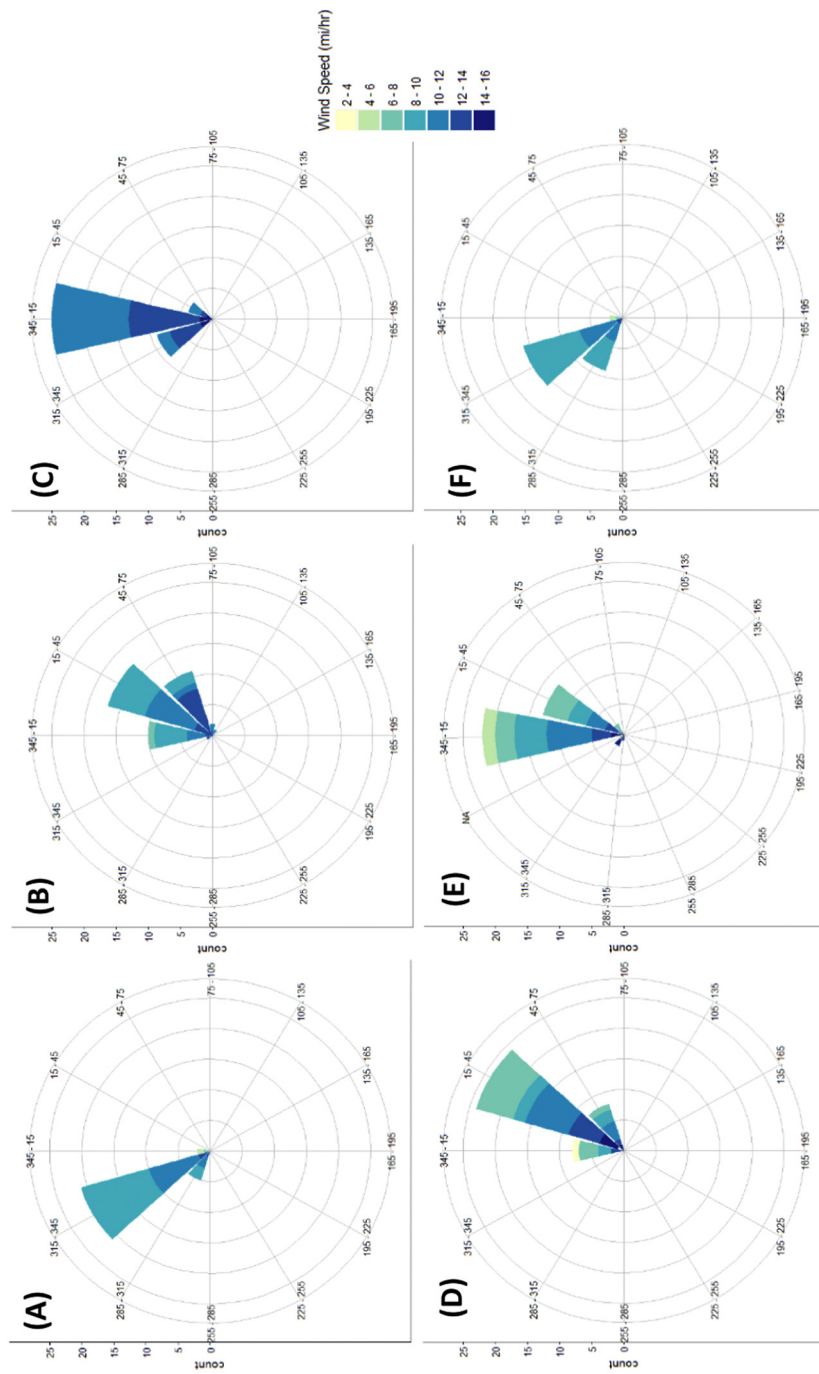


Fig. 11. Wind rose diagrams for aggregated station wind during (A) all observations, (B) rain, (C) snow, (D) mixed precipitation, (E) unknown precipitation, and (F) no precipitation.

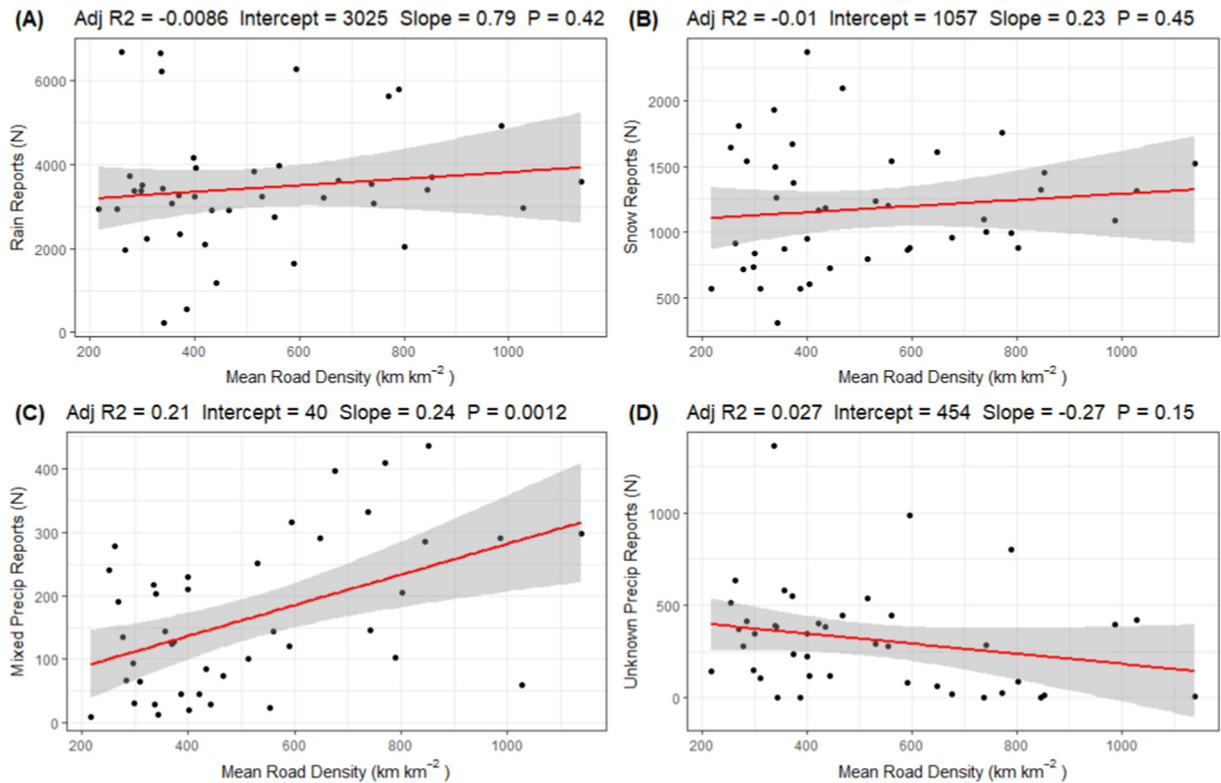


Fig. 12. Linear regression models, $y = Mx + B$, where the dependent variable, y , is station precipitation type total, M is predicted slope (or rate of dependency), x is the station polygon's mean road density, and B is the y-intercept. The models are computed for each precipitation type bin, (A) rain, (B) snow, (C) mixed precipitation, and (D) unknown precipitation. The adjusted R^2 and p -value for each model is shown. The only model with $p < 0.05$ is (C). Shaded regions denote 95% confidence intervals. Note the varying scales on the y-axis in each model.

and are also prohibitive of meaningful analysis on fine spatial scales.

Additional research is necessary to better understand the impact of urbanization on winter precipitation type. This study emphasizes the use of station data. Observation-based studies may include dual polarization radar and hydrometeor classification algorithms which have exhibited the ability to detect all types of winter precipitation (Thompson et al., 2014). The radar network over the current domain has spatial and temporal advantages over the station-based observational network. mPING observations have also been useful in providing ground truth. The relatively static nature of urban growth in developed nations in the last 25 years limits the use of observations to test the evolution of precipitation type over time versus urbanization. Numerical modeling provides a means by which alteration of the urban landscape may be done under identical synoptic conditions. Simulations may be performed to determine atmospheric response to a lack and/or growth of the urban footprint. Lastly, other geographical regions are susceptible to transitional events that cause significant disruptions to commercial activities, infrastructure, and transportation. Providing valuable climatology information to weather forecasters and decision-makers continues to be the primary motivation for the current study and future endeavors.

Funding

This study was supported in part by the National Aeronautics and Space Administration [Grant NNX13AG99G] and the University of Georgia Graduate School.

Conflicts of interest

No other conflicts of interest exist.

Acknowledgements

This paper was funded in combination by National Aeronautics and Space Administration Grant NNX 13AG99G and the University of Georgia Graduate School.

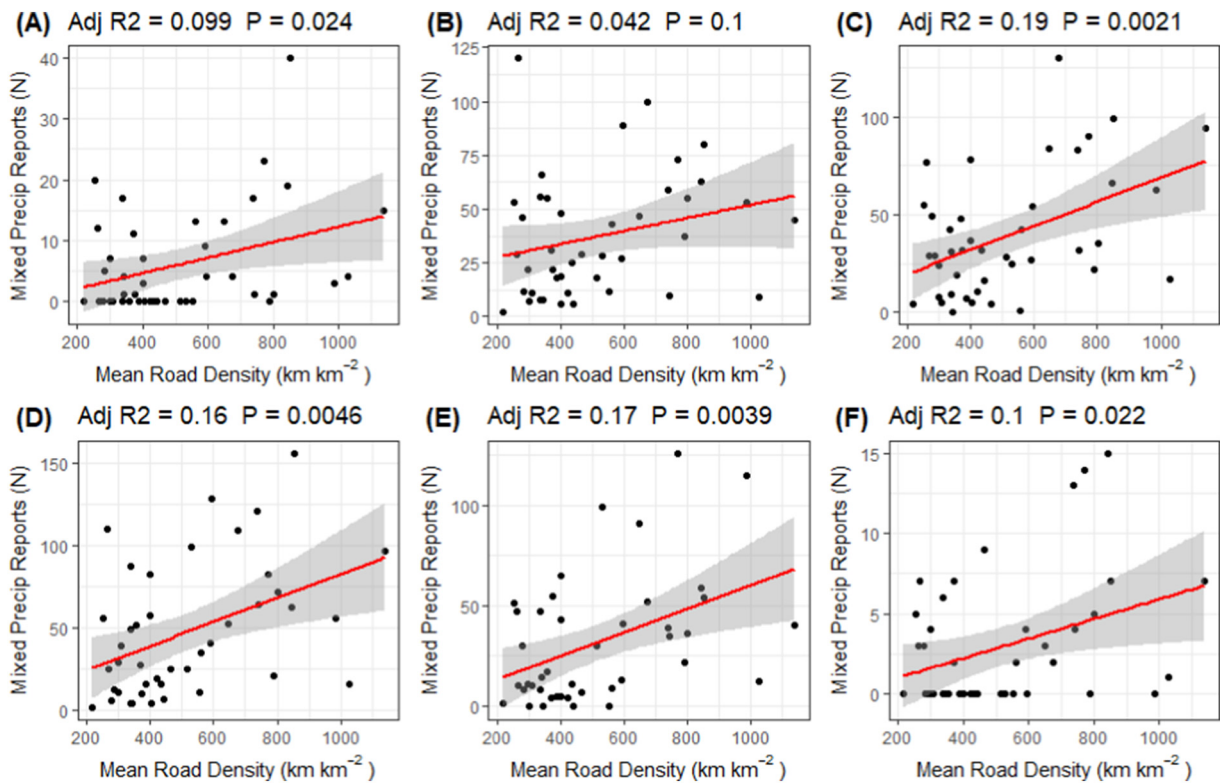


Fig. 13. Linear regression models, $y = Mx + B$, where the dependent variable, y , is station reports of mixed precipitation, M is the predicted slope (or rate of dependency), x is the station polygon's mean road density, and B is the y -intercept. The models are computed for each month, (A) November, (B) December, (C) January, (D) February, (E) March, and (F) April, over the entire temporal span. The adjusted R^2 and p -value for each model is shown. The only model that does not achieve significance ($p < 0.05$) is (B). Shaded regions denote 95% confidence intervals. Note the varying scales on the y -axis in each month.

Appendix A. Supplementary data

Supplementary data to this article can be found online at <https://doi.org/10.1016/j.ulim.2018.03.003>.

References

- Arnfield, A.J., 2003. Two decades of urban climate research: a review of turbulence, exchanges of energy and water, and the urban heat island. *Int. J. Climatol.* 23, 1–26. <http://dx.doi.org/10.1002/joc.859>. <http://doi.wiley.com/10.1002/joc.859>, Accessed date: 25 May 2017.
- Black, A.W., Mote, T.L., 2015. Characteristics of winter-precipitation-related transportation fatalities in the United States. *Weather. Clim. Soc.* 7, 133–145. <http://dx.doi.org/10.1175/WCAS-D-14-00011.1>.
- Changnon, S.A., 2003. Urban modification of freezing-rain events. *J. Appl. Meteorol.* 42, 863–870. [http://dx.doi.org/10.1175/1520-0450\(2003\)042<0863:UMOFE>2.0.CO;2](http://dx.doi.org/10.1175/1520-0450(2003)042<0863:UMOFE>2.0.CO;2).
- Clinton, N., Gong, P., 2013. MODIS detected surface urban heat islands and sinks: global locations and controls. *Remote Sens. Environ.* 134, 294–304. <http://dx.doi.org/10.1016/j.rse.2013.03.008>. <http://www.sciencedirect.com/science/article/pii/S0034425713000874>.
- Cortinas Jr., J.V., Bernstein, B.C., Robbins, C.C., Walter Strapp, J., 2004. An analysis of freezing rain, freezing drizzle, and ice pellets across the United States and Canada: 1976–90. *Weather Forecast.* 19, 377–390. [http://dx.doi.org/10.1175/1520-0434\(2004\)019<0377:AOFRF>2.0.CO;2](http://dx.doi.org/10.1175/1520-0434(2004)019<0377:AOFRF>2.0.CO;2).
- Klein, R.J.T., Nicholls, F., Thomalla, F., Kreimer, A., Arnold, M., Carlin, A., 2003. The resilience of coastal megacities to weather-related hazards. In: *Building Safer Cities: The Future of Disaster Risk*. The World Bank, Washington, DC, pp. 324. <http://dx.doi.org/10.1596/0-8213-5497-3>.
- Luck, M., Wu, J., 2002. A gradient analysis of urban landscape pattern: a case study from the Phoenix metropolitan region, Arizona, USA. *Landsc. Ecol.* 17, 327–339. <http://dx.doi.org/10.1023/A:1020512723753>.
- Maze, T., Agarwai, M., Burchett, G., 2006. Whether weather matters to traffic demand, traffic safety, and traffic operations and flow. *Transp. Res. Rec.* 1948, 170–176. <http://dx.doi.org/10.3141/1948-19>.
- McKinney, M.L., 2002. Urbanization, biodiversity, and conservation: the impacts of urbanization on native species are poorly studied, but educating a highly urbanized human population about these impacts can greatly improve species conservation in all ecosystems. *Bioscience* 52, 883–890. [http://dx.doi.org/10.1641/0006-3568\(2002\)052\[0883:UBAC\]2.0.CO;2](http://dx.doi.org/10.1641/0006-3568(2002)052[0883:UBAC]2.0.CO;2). <http://bioscience.oxfordjournals.org/content/52/10/883.short>.
- McLeod, J., Shepherd, M., Konrad, C.E., 2017. Spatio-temporal rainfall patterns around Atlanta, Georgia and possible relationships to urban land cover. *Urban Clim.* <http://dx.doi.org/10.1016/j.ulim.2017.03.004>. <http://www.sciencedirect.com/science/article/pii/S221209551730024X>, Accessed date: 25 May 2017.
- Mesinger, F., et al., 2006. North American regional reanalysis. *Bull. Am. Meteorol. Soc.* 87, 343–360.
- Mitra, C., Shepherd, J.M., 2016. Urban precipitation: a global perspective. In: Seto, K.C., Solecki, W. (Eds.), *The Routledge Handbook of Urbanization and Global Environment Change*.
- National Centers for Environmental Information, 2017. NOAA/NCEI Quality Controlled Local Climatological Data. <https://www.ncdc.noaa.gov/cdo-web/datasets/lcd>, Accessed date: 8 July 2017.
- National Oceanic and Atmospheric Administration, 1998. Automated Surface Observing System (ASOS) user's guide (61 pp.). <http://www.nws.noaa.gov/asos/pdfs/>

- aum-toc.pdf, Accessed date: 8 July 2017.
- National Oceanic and Atmospheric Administration, 2017. NOAA/ESRL Radiosonde Database. Via University of Wyoming, College of Engineering. <http://weather.uwyo.edu/upperair/sounding.html>, Accessed date: 10 July 2017.
- Oke, T.R., 1995. The Heat Island of the urban boundary layer: characteristics, causes and effects. In: Cermak, J., Davenport, A., Plate, E., Viegas, D. (Eds.), Wind Climate in Cities SE - 5. Vol. 277 of NATO ASI Series Springer Netherlands, pp. 81–107. http://dx.doi.org/10.1007/978-94-017-3686-2_5.
- Reeves, H.D., 2016. The Uncertainty of Precipitation-type Observations and Its Effect on the Validation of Forecast Precipitation Type. <http://dx.doi.org/10.1017/CBO9781107415324.004>.
- Reeves, H.D., Elmore, K.L., Ryzhkov, A., Schuur, T.J., Krause, J., 2014. Sources of uncertainty in precipitation-type forecasting. Weather Forecast. 29, 936–953. <http://dx.doi.org/10.1175/WAF-D-14-00007.1>.
- Schuur, T.J., Park, H.-S., Ryzhkov, A.V., Reeves, H.D., 2012. Classification of precipitation types during transitional winter weather using the RUC model and polarimetric radar retrievals. J. Appl. Meteorol. Climatol. 51, 763–779. <http://dx.doi.org/10.1175/JAMC-D-11-091.1>.
- Seto, K.C., Shepherd, J.M., 2009. Global urban land-use trends and climate impacts. Curr. Opin. Environ. Sustain. 1, 89–95. <http://dx.doi.org/10.1016/j.cosust.2009.07.012>. <http://www.sciencedirect.com/science/article/pii/S1877343509000153>.
- Shepherd, J.M., Mote, T.L., 2011. Can Cities Create Their Own Snowfall? What Observations are Required to Find Out? Earthzine. <http://earthzine.org/2011/09/06/can-cities-create-their-own-snowfall-what-observations-are-required-to-find-out/>.
- Shepherd, J.M., Grundstein, A.J., Mote, T.L., 2014. An analysis of seasonal biases in satellite and reanalysis rainfall products in the Savannah River basin. Phys. Geogr. 35, 181–194. <http://dx.doi.org/10.1080/02723646.2014.887428>.
- Stewart, R.E., King, P., 1987. Freezing precipitation in winter storms. Mon. Weather Rev. 115, 1270–1280. [http://dx.doi.org/10.1175/1520-0493\(1987\)115<1270:FPIWS>2.0.CO;2](http://dx.doi.org/10.1175/1520-0493(1987)115<1270:FPIWS>2.0.CO;2).
- Taha, H., Bornstein, R., 1999. Urbanization of meteorological models and implications on simulated heat islands and air quality. In: Biometeorology and Urban Climatology at the Turn of the Millennium. Selected Papers from the Conference ICB-ICUC '99, Sydney, Australia, pp. 8–12.
- Thériault, J.M., Stewart, R.E., Henson, W., 2010. On the dependence of winter precipitation types on temperature, precipitation rate, and associated features. J. Appl. Meteorol. Climatol. 49, 1429–1442. <http://dx.doi.org/10.1175/2010JAMC2321.1>.
- Thompson, E.J., Rutledge, S.A., Dolan, B., Chandrasekar, V., Cheong, B.L., 2014. A dual-polarization radar hydrometeor classification algorithm for winter precipitation. J. Atmos. Ocean. Technol. 31, 1457–1481. <http://dx.doi.org/10.1175/JTECH-D-13-00119.1>.
- Tobler, W.R., 2004. On the first law of geography: a reply. Ann. Assoc. Am. Geogr. 94, 304–310. <http://dx.doi.org/10.1111/j.1467-8306.2004.09402009.x>.
- United Nations, 2012. World Urbanization Prospects, the 2011 Revision. New York. <http://esa.un.org/unup/Documentation/highlights.htm>, Accessed date: 17 April 2014.
- United States Census Bureau, 2015. 2015 TIGER/Line Shapefiles (machine-readable data files). <https://www.census.gov/geo/maps-data/data/tiger.html>, Accessed date: 10 July 2017.